

Information scrambling and the growth of errors in noisy tomography - a quantum signature of chaos

Abinash Sahu, Naga Dileep Varikuti, and Vaibhav Madhok*

*Department of Physics, Indian Institute of Technology Madras, Chennai, India, 600036 and
Center for Quantum Information, Communication and Computing,
Indian Institute of Technology Madras, Chennai, India 600036*

How does quantum chaos lead to rapid scrambling of information as well as errors across a system when one introduces perturbations in the dynamics? What are its consequences for the reliability of quantum simulations and quantum information processing? We employ continuous measurement quantum tomography as a paradigm to study these questions. The measurement record is generated as a sequence of expectation values of a Hermitian observable evolving under repeated application of the Floquet map of the quantum kicked top. Interestingly, we find that the reconstruction fidelity initially increases regardless of the degree of chaos or the strength of perturbations in the dynamics. For random states, when the measurement record is obtained from a random initial observable, the subsequent drop in the fidelity obtained is inversely correlated to the degree of chaos in the dynamics. More importantly, this also gives us an operational interpretation of Loschmidt echo for operators by connecting it to the performance of quantum tomography. We define a quantity to capture the scrambling of errors, an out-of-time-ordered correlator (OTOC) between two operators under perturbed and unperturbed system dynamics that serves as a signature of chaos and quantifies the spread of errors. Our results demonstrate not only a fundamental link between Loschmidt echo and scrambling of errors, as captured by OTOCs, but that such a link can have operational consequences in quantum information processing.

Chaos, classically as well as in quantum mechanics, has an intimate connection with complexity. Classically, chaos implies unpredictability. Time-evolved trajectories twist and wind away from each other at an exponential rate and then fold back to remain confined in a bounded phase space respecting ergodicity. The flip side of these complex trajectories is the potential information that can be obtained if one tracks these trajectories. The perspective, quantified by the KS (Kolmogorov-Sinai) entropy [1], gives the rate of information gain, at increasingly fine scales, about the missing information in classical chaos - *the initial conditions* [2].

The central goal of quantum chaos is to inform us about the properties of quantum systems whose classical counterpart is chaotic. How does chaos manifest in the quantum world, and what notions of complexity might be suitable to quantify it? Quantum theory comes with another layer of complexity hitherto unknown in our classical description of reality, the Hilbert space, which is a big space [3]. Quantum theory permits the state of the system to be any vector in this space, even permitting a coherent superposition of possibilities considered mutually exclusive in the classical world. Therefore, while classically chaotic dynamics generate classical information in the form of classical trajectories, quantum chaotic dynamics generate quantum information in the form of pseudo-random vectors in the Hilbert space. These states typically have a high entropy which is calculated according to a fixed fiducial basis [4, 5]. Vigorous thrust in the understanding of quantum many-body dynamical systems through dynamically generated entanglement [6–

12] and quantum correlations [13, 14], deeper studies in the ergodic hierarchy of quantum dynamical systems [15–18] have been some recent milestones. Also, the out-of-time-ordered correlators (OTOCs) that attempt to capture operator growth and scrambling of quantum information have been very useful as a probe for chaos in quantum systems [19–26]. These, coupled with the traditional approach to studies of level statistics [27] and Loschmidt echo [28–31] and complemented by the ability to coherently control and manipulate many-body quantum systems in the laboratory [32–36], have brought us to a fork in our path. On the one hand, this is a harbinger of the possibility of building quantum simulators, an important milestone in our quest for the holy grail - a many-body quantum computer. On the other hand, the same properties that make quantum systems generate complexity will make them sensitive to errors that naturally occur in implementing many-body Hamiltonians.

While chaotic dynamics is a source of information quantified by the positive KS entropy, it is sensitive to errors, as captured by Loschmidt echo. In many body systems, quantum or classical, we must expect the presence of both chaos and errors. In this work, we address this scenario; we go on to discover quantum signatures of chaos while shedding light on the larger question of many-body quantum simulations under unavoidable perturbations. While the KS entropy enables a rapid information gain, Loschmidt echo will cause a rapid accumulation of errors, or *error scrambling* as we quantify. This interplay between KS entropy and Loschmidt echo is a generic feature of any many-body system, and we identify and quantify the crossover between these two competing effects.

Quantum tomography gives us a window to study

* madhok@physics.iitm.ac.in

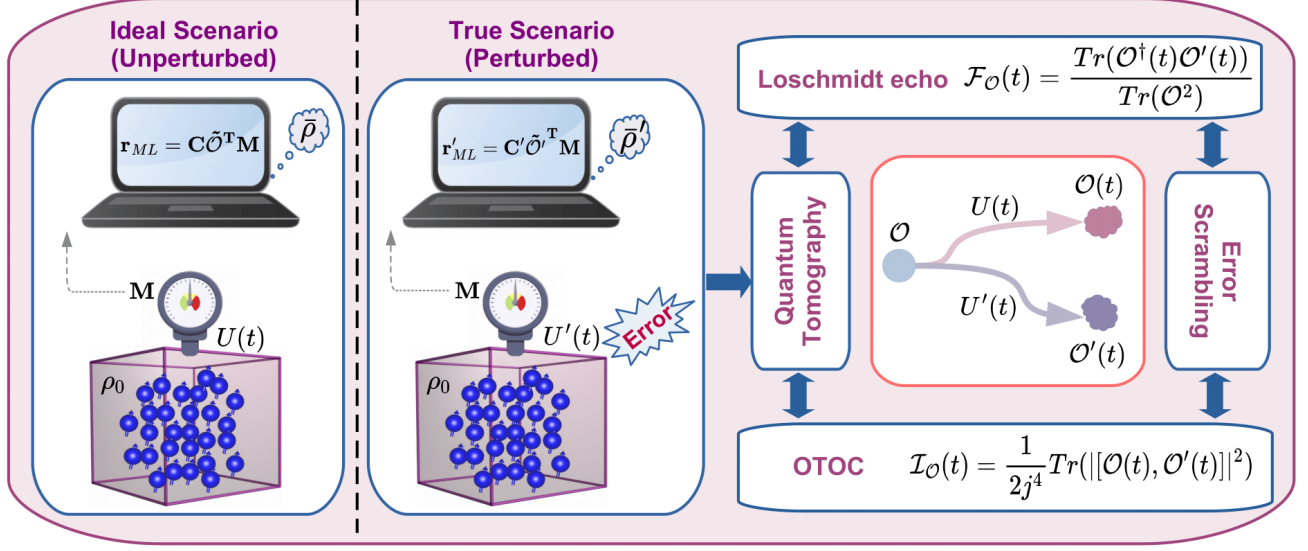


FIG. 1. An illustration of continuous measurement tomography and its connection with various quantifiers of quantum chaos. In the ideal scenario where the experimentalist has complete knowledge of the true dynamics, the reconstructed state reaches the actual state with time. However, in reality, the experimentalist is ignorant about the true (perturbed) dynamics that leads to improper reconstruction of the quantum state. Thus, the reconstruction fidelity decays after some time and positively correlates with the operator Loschmidt echo. We quantify the scrambling of error as $\mathcal{I}_{\mathcal{O}}(t)$, and it helps to unify Loschmidt echo $\mathcal{F}_{\mathcal{O}}(t)$ and OTOC in a real quantum information processing task, quantum tomography.

sensitivity to errors in quantum simulations of chaotic Hamiltonians [37, 38]. Quantum tomography uses the statistics of measurement records on an ensemble of identical systems in order to make the best estimate of the actual state ρ_0 . We consider continuous weak measurement tomography protocol [35, 39–41], and the time series of operators can be generated by the Floquet map of a quantum dynamical system to investigate the role of chaos on the information gain in tomography [42–44]. Here we unify two quantifiers of quantum chaos, namely Loschmidt echo and OTOC, through scrambling of errors in continuous weak measurement tomography as illustrated in Fig. 1.

An ensemble of N identical systems $\rho_0^{\otimes N}$ undergo separable time evolution by a unitary $U(t)$. A weakly coupled probe will generate the measurement record by performing weak continuous measurement of an observable \mathcal{O} . For sufficiently weak coupling, the randomness of the measurement outcomes is dominated by the quantum noise in the probe rather than the measurement uncertainty, i.e., the projection noise. In this case, the quantum backaction is negligible, and the state remains approximately separable. Thus, we get the stochastic measurement record

$$M(t) = \text{Tr}(\mathcal{O}(t)\rho_0) + W(t), \quad (1)$$

where $\mathcal{O}(t) = U^\dagger(t)\mathcal{O}U(t)$ is the time evolved operator in Heisenberg picture, and $W(t)$ is a Gaussian white noise with spread σ/N .

Any density matrix of Hilbert-space dimension d can

be realized as a generalized Bloch vector \mathbf{r} by expanding $\rho_0 = I/d + \sum_{\alpha=1}^{d^2-1} r_\alpha E_\alpha$ in an orthonormal basis of traceless Hermitian operators $\{E_\alpha\}$. We consider the measurement record at discrete times as $M_n = M(t_n) = \text{Tr}(\mathcal{O}_n\rho_0) + W_n$, that allows one to express the measurement history

$$\mathbf{M} = \tilde{\mathcal{O}}\mathbf{r} + \mathbf{W}, \quad (2)$$

where $\tilde{\mathcal{O}}_{n\alpha} = \text{Tr}(\mathcal{O}_n E_\alpha)$. Thus, the problem of quantum tomography is reduced to linear stochastic state estimation of ρ_0 given $\{M_n\}$. In the limit of negligible backaction, the probability distribution associated with measurement history \mathbf{M} for a given state vector \mathbf{r} is [39, 40]

$$\begin{aligned} p(\mathbf{M}|\mathbf{r}) &\propto \exp\left\{-\frac{N^2}{2\sigma^2}\sum_i[M_i - \sum_\alpha \tilde{\mathcal{O}}_{i\alpha}r_\alpha]^2\right\} \\ &\propto \exp\left\{-\frac{N^2}{2\sigma^2}\sum_{\alpha,\beta}(\mathbf{r} - \mathbf{r}_{\text{ML}})_\alpha C_{\alpha\beta}^{-1}(\mathbf{r} - \mathbf{r}_{\text{ML}})_\beta\right\}. \end{aligned} \quad (3)$$

In the weak backaction limit, the fluctuations around the mean are Gaussian distributed, and hence the maximum likelihood estimate of the Bloch vector components is the least-squared fit as

$$\mathbf{r}_{\text{ML}} = \mathbf{C}\tilde{\mathcal{O}}^T\mathbf{M}, \quad (4)$$

where $\mathbf{C} = (\tilde{\mathcal{O}}^T\tilde{\mathcal{O}})^{-1}$ is the covariance matrix and the inverse is Moore-Penrose pseudo inverse [45] in general.

The estimated Bloch vector \mathbf{r}_{ML} may not always represent a physical density matrix with non-negative eigenvalues because of the finite signal-to-noise ratio. Therefore we impose the constraint of positive semidefiniteness on the reconstructed density matrix and obtain the physical state closest to the maximum-likelihood estimate. To do this, we employ a convex optimization procedure [46] where the final estimate of the Bloch vector $\bar{\mathbf{r}}$ is obtained by minimizing the argument

$$\|\mathbf{r}_{ML} - \bar{\mathbf{r}}\|^2 = (\mathbf{r}_{ML} - \bar{\mathbf{r}})^T \mathbf{C}^{-1} (\mathbf{r}_{ML} - \bar{\mathbf{r}}) \quad (5)$$

subject to the constraint

$$I/d + \sum_{\alpha=1}^{d^2-1} \bar{r}_\alpha E_\alpha \geq 0.$$

The above description represents an ideal scenario where the experimentalist has complete knowledge of the *true* dynamics (which is symbolized as unprimed variables describing the observables, \mathcal{O}_n , and covariance matrix, \mathbf{C} , thus generated over time) and they can properly reconstruct the state using Eq. (4). However, in reality, one never knows the true underlying dynamics, and there is always a departure from the ideal case due to inevitable errors and perturbations to the *true* dynamics. Thus, the experimentalist, oblivious to these, models their estimation using a covariance matrix, $\mathbf{C}' = (\tilde{\mathcal{O}}'^T \tilde{\mathcal{O}}')^{-1}$. Here the primed variables represent the experimentalist's knowledge of the dynamics in the laboratory, and as a result, they end up reconstructing an incorrect state as $\bar{\rho}'$ from

$$\mathbf{r}'_{ML} = \mathbf{C}' \tilde{\mathcal{O}}'^T \mathbf{M}. \quad (6)$$

In the above equation, the measurement record is obtained from the measurement device (probe), and the experimentalist is ignorant about the *true* dynamics (which is accompanied by perturbations relative to the idealized dynamics as assumed by the experimentalist), given by the unitary $U(t)$, that has generated this record. However, the covariance matrix is uniquely determined from the experimentalist's version of the dynamics given by the unitary $U'(t)$ and the initial observable \mathcal{O} . Thus, the ignorance about the error in the dynamics directs the operator trajectory away from the actual one, leading to an improper reconstruction of the state ρ_0 .

Our goal is to study the effect of the perturbation on the information gain in tomography in the presence of chaos. To accomplish this, we implement the quantum kicked top [27, 47, 48] described by the Floquet map $F_{QKT} = e^{-i\lambda J_z^2/2J} e^{-i\alpha J_x}$ as the unitary for a period τ for simplicity, and the unitary at n^{th} time step is $U(n\tau) = U_\tau^n$. The measurement record generated by such periodic application of the Floquet map is not informationally complete, and it leaves out a subspace of dimension $\geq d - 2$, out of $d^2 - 1$ dimensional operator space. For our current work, we fix the linear precision angle $\alpha = 1.4$ and choose the kicking strength

λ as the chaoticity parameter. The classical dynamics change from highly regular to fully chaotic as we vary λ from 0 to 7. The dynamics that represents the *true* evolution is perturbed relative to the idealized dynamics given by F_{QKT} , and we choose a small variation in the kicking strength, $\lambda + \delta\lambda$, and the perturbed unitary becomes $U_\tau = e^{-i(\lambda+\delta\lambda)J_z^2/2J} e^{-i\alpha J_x}$. For our analysis, we consider the dynamics of quantum kicked top for a spin $j = 10$, and perturbation strength $\delta\lambda = 0.01$.

The connection between chaos and information gain depends on the localization properties of the state, i.e. their inverse participation ratio, the degree of chaos, as well as how well the state is aligned with time-evolved measurement observables [44]. Therefore, to study the effect of the degree of chaos on the performance of noisy tomography purely, we consider random initial states measured via random initial observables (generated by rotating J_x through random unitary) picked from the appropriate Haar measure. We apply our reconstruction protocol on an ensemble of 100 random pure states sampled from the Haar measure on $SU(d)$, where $d = 2j + 1 = 21$. We choose one random initial observable and generate the measurement record from the repeated application of the Floquet map of the quantum kicked top. The fidelity of the reconstructed state $\bar{\rho}'$ obtained from Eq. (6) is determined relative to the actual state $|\psi_0\rangle$, $\mathcal{F} = \langle \psi_0 | \bar{\rho}' | \psi_0 \rangle$ as a function of time. We notice that the reconstruction fidelity increases in the beginning despite the errors, and after a certain period of time, it starts decaying. The rise in fidelity during the initial time period is because any information, even if partially inaccurate, about a completely unknown random state offsets the presence of errors in its estimation. However, as time progresses, the effect of errors becomes significant. Beyond a certain time, we observe a decline in fidelity as the dynamics continues to accumulate errors that dominate the archive of information present in the measurement record. Most interestingly, the rate of this fidelity decay is inversely correlated with the degree of chaos in the dynamics. This is the analog of an interplay between the rapid information gain due to Lyapunov divergence, a ‘‘quantum’’ analog of the classical KS entropy, and Loschmidt echo leading to errors that cause fidelity decay.

We now quantify the role of chaos in tomography when the error in the dynamics influences our ability to reconstruct the random quantum states. It is evident from Fig. 2a that the rate of drop in fidelity decreases with an increase in the strength of chaos for small perturbations in the dynamics. To understand the foregoing discussion, we define the operator Loschmidt echo $\mathcal{F}_\mathcal{O}$ as the Hilbert-Schmidt inner product of the operators \mathcal{O}_n , and \mathcal{O}'_n generated from repeated application of the Floquet map for *true* (perturbed) dynamics U_τ and ideal (unperturbed) dynamics U'_τ of the kicked top on the initial observable \mathcal{O}

$$\mathcal{F}_\mathcal{O}(t_n) = \frac{\text{Tr}(\mathcal{O}_n^\dagger \mathcal{O}'_n)}{\text{Tr}(\mathcal{O}^2)}. \quad (7)$$

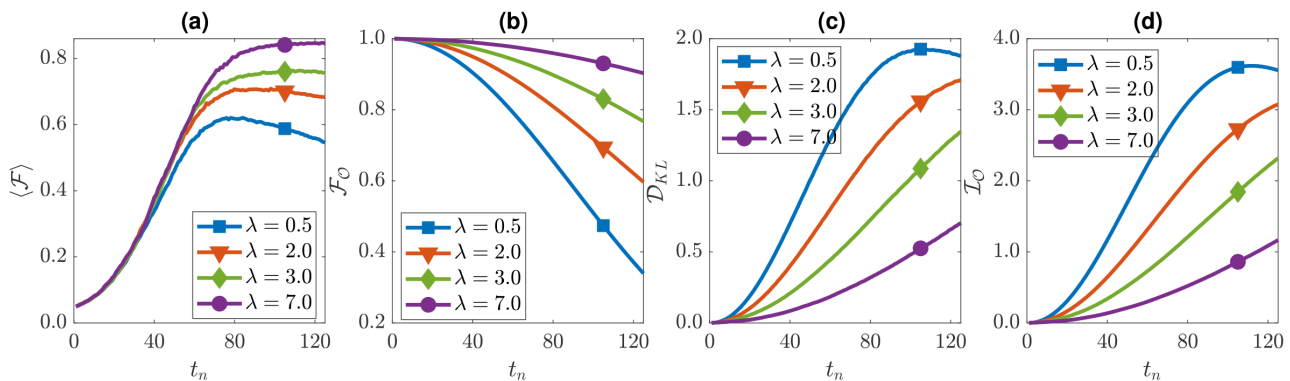


FIG. 2. Effect of perturbation on tomography quantified by different metrics as a function of time with an increase in the level of chaos. The kicked top Floquet map of *true* (perturbed) dynamics $U_\tau = e^{-i(\lambda+\delta\lambda)J_z^2/2J} e^{-i\alpha J_x}$ with $\delta\lambda = 0.01$, and ideal (unperturbed) dynamics $U'_\tau = e^{-i\lambda J_z^2/2J} e^{-i\alpha J_x}$ generate the time series of operators for a spin $j = 10$ and fixed $\alpha = 1.4$. (a) Average reconstruction fidelity $\langle \mathcal{F} \rangle$ of the state $\bar{\rho}'$ derived from Eq. (6) relative to the actual state $|\psi_0\rangle$, where the average is taken over 100 Haar random states. (b) The operator Loschmidt echo \mathcal{F}_O between two operators. (c) The quantum relative entropy \mathcal{D}_{KL} of regularized operator evolved under unperturbed dynamics to the operator evolved under perturbed dynamics. (d) The operator incompatibility \mathcal{I}_O quantifies the scrambling of errors.

The operator Loschmidt echo that captures the overlap of the operators \mathcal{O}_n and \mathcal{O}'_n , decays with time. We can see from Fig. 2b that the operator Loschmidt echo decays much slower when the dynamics is chaotic than when it is regular. This behavior of the operator Loschmidt echo correlates positively with the rate of drop in reconstruction fidelity as demonstrated in Fig. 2a and Fig. 2b. The greater the distance between the operators at a given time, the greater the difference between the expectation values with respect to the state and the archive of the measurement record obtained through the time series. Our results give an *operational interpretation* of the operator Loschmidt echo by connecting it to a concrete physical task of continuous measurement quantum tomography. This also points to a beneficial way to probe these quantities in experiments using current techniques. Quantum relative entropy is a measure of distance between two quantum states. Here we use this metric to measure the distance between two operators \mathcal{O}_n and \mathcal{O}'_n . To treat both observables as density operators, we regularize them as follows. We construct a positive operator from an observable by retaining its eigenvectors and taking the absolute value of its eigenvalues. To normalize this operator, we divide it by its trace [see Methods for details]. Now we can determine the quantum relative entropy

$$\mathcal{D}_{KL}(\rho_{\mathcal{O}_n} || \rho_{\mathcal{O}'_n}) = \text{Tr}(\rho_{\mathcal{O}_n}(\log \rho_{\mathcal{O}_n} - \log \rho_{\mathcal{O}'_n})), \quad (8)$$

where $\rho_{\mathcal{O}_n}$ and $\rho_{\mathcal{O}'_n}$ are positive operators of unit trace obtained from the regularization of operators \mathcal{O}_n and \mathcal{O}'_n respectively. We can see clearly from Fig. 2c that the distance between the two operators increases rapidly when the level of chaos is less in the dynamics. This indicates the operator becomes less prone to error in the Hamiltonian with the rise in the level of chaos. Ultimately, this makes quantum state tomography more immune to error

in the presence of chaos, as we see in Fig. 2a.

To further elucidate the decline rate of reconstruction fidelity, we connect the operator incompatibility to the information gain. We quantify the incompatibility of two operators \mathcal{O}_n and \mathcal{O}'_n with time as $\mathcal{I}_O(t_n) = \frac{1}{2j^4} \text{Tr}(|[\mathcal{O}_n, \mathcal{O}'_n]|^2)$. Interestingly, \mathcal{I}_O can be realized as a quantity like OTOC evolved under an effective *error unitary* $\mathcal{U}_n = U_\tau'^n U_\tau^{\dagger n}$

$$\mathcal{I}_O(t_n) = \frac{1}{2j^4} \text{Tr}(|[\mathcal{O}, \mathcal{U}_n^\dagger \mathcal{O} \mathcal{U}_n]|^2). \quad (9)$$

This form of error scrambling is very general for dynamics with time-dependent as well as time-independent Hamiltonian [see Methods for details]. The growth of OTOC has been studied extensively as a quantifier for information scrambling under chaotic dynamics [19–26]. Similarly, growth of \mathcal{I}_O implies *scrambling of errors* with time. It is apparent from Fig. 2d that the rate of error scrambling decreases with an increase in the value of the chaoticity parameter λ . This signifies that the measurement record is less affected by the error in the dynamics when one approaches a greater extent of chaos. In Eq. (6), the measurement record \mathbf{M} is obtained from the *true* (perturbed) dynamics, but the covariance matrix \mathbf{C}' , and \mathcal{O}' are determined from the experimentalist's version of the dynamics (ideal or unperturbed). Thus, a higher rate of error scrambling for regular dynamics leads to a faster decay of reconstruction fidelity as the measurement record is more vulnerable. How errors scramble across a chaotic system, as given by Eq. (9), is itself an interesting quantifier of quantum chaos. Here we notice the correlation between scrambling of errors as captured by the incompatibility between the operator and its time evolution through the *error unitary* in Eq. (9) and operator Loschmidt echo, as viewed from the lens of quantum tomography under chaotic dynamics. This links two

fundamental quantifiers of quantum chaos, complements findings in [49] and provides a different but more intuitive connection.

We find dynamical signatures of chaos that quantify the scrambling of errors across a many-body quantum system that has consequences on the performance of quantum information and simulation protocols. We also give an operational interpretation of the operator Loschmidt echo by connecting it to the growth of distance between operators evolved in continuous measurement quantum tomography. Our results linking Loschmidt echo, error scrambling, and OTOCs will be helpful to the condensed matter community as well and in addressing broader issues involving non-integrable quantum systems [50].

Our work paves the way for further studies in the performance of quantum simulations under inadvertent noise. In the era of noisy, intermediate-scale quantum (NISQ) devices [51], the accuracy of an analog quantum simulator will decay after just a few time steps. The reliability of such analog quantum simulators is highly questionable even for state-of-the-art architecture when it is likely to exhibit quantum chaos [52, 53]. On the contrary, the digital quantum simulation is often associated with the inherent Trotter errors [54] because of the

discretization of the time evolution of a quantum many-body system as a sequence of quantum gates. Thus, a better understanding of errors in simulating many-body quantum systems and information processing protocols that exploit such rich dynamics is paramount. These signatures of chaos can be further explored using state-of-the-art experimental techniques involving cold atoms interacting with lasers and magnetic fields [48]. In future work, we hope to further build upon our results to develop quantum analogs of the “classical shadowing lemma” that guarantee a *true* classical trajectory in the neighbourhood of any arbitrary simulated trajectory of a chaotic system in the presence of truncation errors due to finite precision [55–59].

We are grateful to Arul Lakshminarayan for useful discussions. We thank Sreeram PG for helpful discussions. We acknowledge BS Datta Vikas for his inputs during the initial stage of this work. The authors would like to thank HPCE, IIT Madras, for providing the computational facility for numerical simulations. This work was supported in part by grant DST/ICPS/QuST/Theme-3/2019/Q69 and New faculty Seed Grant from IIT Madras. The authors were supported, in part, by a grant from Mphasis to the Centre for Quantum Information, Communication, and Computing (CQuICC) at IIT Madras.

-
- [1] Ya B Pesin. Characteristic lyapunov exponents and smooth ergodic theory. *Russian Mathematical Surveys*, 32(4):55, 1977.
- [2] Carlton M. Caves and Rüdiger Schack. Unpredictability, information, and chaos. *Complexity*, 3(1):46–57, 1997.
- [3] Carlton M Caves and Christopher A Fuchs. Quantum information: How much information in a state vector? *arXiv preprint quant-ph/9601025*, 1996.
- [4] William K Wootters. Random quantum states. *Foundations of Physics*, 20(11):1365–1378, 1990.
- [5] Ingemar Bengtsson and Karol Życzkowski. *Geometry of quantum states: an introduction to quantum entanglement*. Cambridge university press, 2017.
- [6] Paul A Miller and Sarben Sarkar. Signatures of chaos in the entanglement of two coupled quantum kicked tops. *Physical Review E*, 60(2):1542, 1999.
- [7] Jayendra N Bandyopadhyay and Arul Lakshminarayan. Testing statistical bounds on entanglement using quantum chaos. *Physical review letters*, 89(6):060402, 2002.
- [8] Xiaoguang Wang, Shohini Ghose, Barry C Sanders, and Bambi Hu. Entanglement as a signature of quantum chaos. *Physical Review E*, 70(1):016217, 2004.
- [9] Collin M Trail, Vaibhav Madhok, and Ivan H Deutsch. Entanglement and the generation of random states in the quantum chaotic dynamics of kicked coupled tops. *Physical Review E*, 78(4):046211, 2008.
- [10] K Furuya, MC Nemes, and GQ Pellegrino. Quantum dynamical manifestation of chaotic behavior in the process of entanglement. *Physical review letters*, 80(25):5524, 1998.
- [11] Arul Lakshminarayan. Entangling power of quantized chaotic systems. *Physical Review E*, 64(3):036207, 2001.
- [12] Akshay Seshadri, Vaibhav Madhok, and Arul Lakshminarayan. Tripartite mutual information, entanglement, and scrambling in permutation symmetric systems with an application to quantum chaos. *Physical Review E*, 98(5):052205, 2018.
- [13] Vaibhav Madhok, Vibhu Gupta, Denis-Alexandre Trotter, and Shohini Ghose. Signatures of chaos in the dynamics of quantum discord. *Physical Review E*, 91(3):032906, 2015.
- [14] Vaibhav Madhok, Shruti Dogra, and Arul Lakshminarayan. Quantum correlations as probes of chaos and ergodicity. *Optics Communications*, 420:189–193, 2018.
- [15] Ignacio Gomez and Mario Castagnino. Towards a definition of the quantum ergodic hierarchy: Kolmogorov and bernoulli systems. *Physica A: Statistical Mechanics and its Applications*, 393:112–131, 2014.
- [16] Bruno Bertini, Pavel Kos, and Tomaž Prosen. Exact correlation functions for dual-unitary lattice models in 1+ 1 dimensions. *Physical review letters*, 123(21):210601, 2019.
- [17] S Aravinda, Suhail Ahmad Rather, and Arul Lakshminarayan. From dual-unitary to quantum bernoulli circuits: Role of the entangling power in constructing a quantum ergodic hierarchy. *Physical Review Research*, 3(4):043034, 2021.
- [18] Amit Vikram and Victor Galitski. Dynamical quantum ergodicity from energy level statistics. *arXiv preprint arXiv:2205.05704*, 2022.
- [19] Juan Maldacena, Stephen H Shenker, and Douglas Stanford. A bound on chaos. *Journal of High Energy Physics*, 2016(8):1–17, 2016.
- [20] Brian Swingle, Gregory Bentsen, Monika Schleier-Smith,

- and Patrick Hayden. Measuring the scrambling of quantum information. *Physical Review A*, 94(4):040302, 2016.
- [21] Koji Hashimoto, Keiju Murata, and Ryosuke Yoshii. Out-of-time-order correlators in quantum mechanics. *Journal of High Energy Physics*, 2017(10):1–31, 2017.
- [22] Ivan Kukuljan, Sašo Grozdanov, and Tomaž Prosen. Weak quantum chaos. *Physical Review B*, 96(6):060301, 2017.
- [23] Brian Swingle. Unscrambling the physics of out-of-time-order correlators. *Nature Physics*, 14(10):988–990, 2018.
- [24] Jiaozhi Wang, Giuliano Benenti, Giulio Casati, and Wenge Wang. Quantum chaos and the correspondence principle. *Physical Review E*, 103(3):L030201, 2021.
- [25] PG Sreeram, Vaibhav Madhok, and Arul Lakshminarayan. Out-of-time-ordered correlators and the loschmidt echo in the quantum kicked top: how low can we go? *Journal of Physics D: Applied Physics*, 54(27):274004, 2021.
- [26] Naga Dileep Varikuti and Vaibhav Madhok. Out-of-time ordered correlators in kicked coupled tops and the role of conserved quantities in information scrambling. *arXiv preprint arXiv:2201.05789*, 2022.
- [27] F. Haake. *Quantum Signatures of Chaos*. Springer-Verlag, Berlin, 1991.
- [28] Asher Peres. Stability of quantum motion in chaotic and regular systems. *Physical Review A*, 30(4):1610, 1984.
- [29] Asher Peres. *Quantum theory: concepts and methods*. Springer, 1997.
- [30] A. Goussev, R. A. Jalabert, H. M. Pastawski, and D. Ariel Wisniacki. Loschmidt echo. *Scholarpedia*, 7(8):11687, 2012.
- [31] Thomas Gorin, Tomaž Prosen, Thomas H Seligman, and Marko Žnidarič. Dynamics of loschmidt echoes and fidelity decay. *Physics Reports*, 435(2-5):33–156, 2006.
- [32] Jiangbin Gong and Paul Brumer. Coherent control of quantum chaotic diffusion: Diatomic molecules in a pulsed microwave field. *The Journal of Chemical Physics*, 115(8):3590–3597, 2001.
- [33] Jiangbin Gong and Paul Brumer. Quantum chaos meets coherent control. *Annual review of physical chemistry*, 56:1, 2005.
- [34] Constantin Brif, Raj Chakrabarti, and Herschel Rabitz. Control of quantum phenomena: past, present and future. *New Journal of Physics*, 12(7):075008, 2010.
- [35] A Smith, CA Riofrío, BE Anderson, H Sosa-Martinez, IH Deutsch, and PS Jessen. Quantum state tomography by continuous measurement and compressed sensing. *Physical Review A*, 87(3):030102, 2013.
- [36] Nicolás Mirkin and Diego Wisniacki. Quantum chaos, equilibration, and control in extremely short spin chains. *Physical Review E*, 103(2):L020201, 2021.
- [37] Seth Lloyd. Universal quantum simulators. *Science*, 273(5278):1073–1078, 1996.
- [38] Tomi H. Johnson, Stephen R. Clark, and Dieter Jaksch. What is a quantum simulator? *EPJ Quantum Technology*, 1(1):10, Jul 2014.
- [39] Andrew Silberfarb, Poul S Jessen, and Ivan H Deutsch. Quantum state reconstruction via continuous measurement. *Physical review letters*, 95(3):030402, 2005.
- [40] Greg A Smith, Andrew Silberfarb, Ivan H Deutsch, and Poul S Jessen. Efficient quantum-state estimation by continuous weak measurement and dynamical control. *Physical review letters*, 97(18):180403, 2006.
- [41] Carlos A Riofrío, Poul S Jessen, and Ivan H Deutsch. Quantum tomography of the full hyperfine manifold of atomic spins via continuous measurement on an ensemble. *Journal of Physics B: Atomic, Molecular and Optical Physics*, 44(15):154007, 2011.
- [42] Vaibhav Madhok, Carlos A Riofrío, Shohini Ghose, and Ivan H Deutsch. Information gain in tomography—a quantum signature of chaos. *Physical review letters*, 112(1):014102, 2014.
- [43] PG Sreeram and Vaibhav Madhok. Quantum tomography with random diagonal unitary maps and statistical bounds on information generation using random matrix theory. *Physical Review A*, 104(3):032404, 2021.
- [44] Abinash Sahu, PG Sreeram, and Vaibhav Madhok. Effect of chaos on information gain in quantum tomography. *Physical Review E*, 106(2):024209, 2022.
- [45] Adi Ben-Israel and Thomas NE Greville. *Generalized inverses: theory and applications*, volume 15. Springer Science & Business Media, 2003.
- [46] Lieven Vandenbergh and Stephen Boyd. Semidefinite programming. *SIAM review*, 38(1):49–95, 1996.
- [47] Fritz Haake, M Kuś, and Rainer Scharf. Classical and quantum chaos for a kicked top. *Zeitschrift für Physik B Condensed Matter*, 65(3):381–395, 1987.
- [48] S Chaudhury, A Smith, BE Anderson, S Ghose, and Poul S Jessen. Quantum signatures of chaos in a kicked top. *Nature*, 461(7265):768–771, 2009.
- [49] Bin Yan, Lukasz Cincio, and Wojciech H. Zurek. Information scrambling and loschmidt echo. *Phys. Rev. Lett.*, 124:160603, Apr 2020.
- [50] Mohit Pandey, Pieter W Claeys, David K Campbell, Anatoli Polkovnikov, and Dries Sels. Adiabatic eigenstate deformations as a sensitive probe for quantum chaos. *Physical Review X*, 10(4):041017, 2020.
- [51] John Preskill. Quantum computing in the nisq era and beyond. *Quantum*, 2:79, 2018.
- [52] Philipp Hauke, Fernando M Cucchietti, Luca Tagliacozzo, Ivan Deutsch, and Maciej Lewenstein. Can one trust quantum simulators? *Reports on Progress in Physics*, 75(8):082401, 2012.
- [53] Nathan K Lysne, Kevin W Kuper, Pablo M Poggi, Ivan H Deutsch, and Poul S Jessen. Small, highly accurate quantum processor for intermediate-depth quantum simulations. *Physical review letters*, 124(23):230501, 2020.
- [54] Markus Heyl, Philipp Hauke, and Peter Zoller. Quantum localization bounds trotter errors in digital quantum simulation. *Science advances*, 5(4):eaau8342, 2019.
- [55] Dmitry Victorovich Anosov. Geodesic flows on closed riemannian manifolds of negative curvature. *Trudy Matematicheskogo Instituta Imeni VA Steklova*, 90:3–210, 1967.
- [56] Celso Grebogi, Stephen M Hammel, James A Yorke, and Tim Sauer. Shadowing of physical trajectories in chaotic dynamics: Containment and refinement. *Physical Review Letters*, 65(13):1527, 1990.
- [57] Tim Sauer and James A Yorke. Rigorous verification of trajectories for the computer simulation of dynamical systems. *Nonlinearity*, 4(3):961, 1991.
- [58] Tim Sauer, Celso Grebogi, and James A Yorke. How long do numerical chaotic solutions remain valid? *Physical Review Letters*, 79(1):59, 1997.
- [59] Jiří Vaníček. Dephasing representation: Employing the shadowing theorem to calculate quantum correlation functions. *Physical Review E*, 70(5):055201, 2004.
- [60] Seth T Merkel, Carlos A Riofrío, Steven T Flammia, and Ivan H Deutsch. Random unitary maps for quantum

state reconstruction. *Physical Review A*, 81(3):032126, 2010.

Derivation of Error scrambling expression

SUPPLEMENTARY MATERIAL

Relative entropy calculation

While calculating the relative entropy, we regularize the operator in the following way. First, we diagonalize the time-evolved operator \mathcal{O}_n as

$$\mathcal{O}_n = V_n D_n V_n^\dagger, \quad (10)$$

where V_n is the unitary matrix that diagonalizes \mathcal{O}_n . In the second step, we take the absolute value of the eigenvalues of D_n and divide it by its trace to get $\tilde{D}_n = |D_n|/\text{Tr}(|D_n|)$. We, then, construct a positive operator with unit trace that behaves as a density matrix while keeping the eigenvectors of the observable \mathcal{O}_n intact as

$$\rho_{\mathcal{O}_n} = V_n \tilde{D}_n V_n^\dagger. \quad (11)$$

Now we can calculate the quantum relative entropy between the two operators \mathcal{O}_n and \mathcal{O}'_n as

$$\mathcal{D}_{KL}(\rho_{\mathcal{O}_n} || \rho_{\mathcal{O}'_n}) = \text{Tr}(\rho_{\mathcal{O}_n}(\log \rho_{\mathcal{O}_n} - \log \rho_{\mathcal{O}'_n})). \quad (12)$$

$$\begin{aligned} \text{Tr}(|[\mathcal{O}(t), \mathcal{O}'(t)]|^2) &= \text{Tr}([\mathcal{O}(t), \mathcal{O}'(t)]^\dagger [\mathcal{O}(t), \mathcal{O}'(t)]) \\ &= \text{Tr}\left(\left((\mathcal{O}(t)\mathcal{O}'(t) - \mathcal{O}'(t)\mathcal{O}(t))^\dagger (\mathcal{O}(t)\mathcal{O}'(t) - \mathcal{O}'(t)\mathcal{O}(t))\right)\right) \\ &= \text{Tr}\left(\left((\mathcal{O}'(t)\mathcal{O}(t) - \mathcal{O}(t)\mathcal{O}'(t))(\mathcal{O}(t)\mathcal{O}'(t) - \mathcal{O}'(t)\mathcal{O}(t))\right)\right) \\ &= \text{Tr}\left(\left(\mathcal{O}'(t)\mathcal{O}(t)\mathcal{O}(t)\mathcal{O}'(t) - \mathcal{O}'(t)\mathcal{O}(t)\mathcal{O}'(t)\mathcal{O}(t) - \mathcal{O}(t)\mathcal{O}'(t)\mathcal{O}(t)\mathcal{O}'(t) + \mathcal{O}(t)\mathcal{O}'(t)\mathcal{O}'(t)\mathcal{O}(t)\right)\right) \end{aligned} \quad (14)$$

We can further simplify the above expression by exploiting the cyclic property of trace operation and the prop-

The operator incompatibility we have computed for the operators evolved through unperturbed and perturbed dynamics. This form is very general, and we do not assume any specific form of the error or any particular form of Hamiltonian (whether time-dependent or time-independent), as we can see below. Let the operators at time t be $\mathcal{O}(t) = U^\dagger(t)\mathcal{O}U(t)$ and $\mathcal{O}'(t) = U'^\dagger(t)\mathcal{O}'U'(t)$, where $U(t)$ is the unitary for the unperturbed dynamics and $U'(t)$ is the unitary for perturbed dynamics. Thus, the operator incompatibility is

$$\mathcal{I}_{\mathcal{O}}(t) = \frac{1}{2j^4} \text{Tr}(|[\mathcal{O}(t), \mathcal{O}'(t)]|^2). \quad (13)$$

Now one can simplify this expression using the Hermiticity property of the physical observables $\mathcal{O}(t) = \mathcal{O}^\dagger(t)$.

erty of a unitary operator $U^\dagger U = U U^\dagger = \mathbb{1}$. Let us consider the first term in the above expression

$$\begin{aligned} \text{Tr}\left(\mathcal{O}'(t)\mathcal{O}(t)\mathcal{O}(t)\mathcal{O}'(t)\right) &= \text{Tr}\left(U'^\dagger(t)\mathcal{O}'U'(t)U^\dagger(t)\mathcal{O}U(t)U^\dagger(t)\mathcal{O}U(t)U'^\dagger(t)\mathcal{O}'U'(t)\right) \\ &= \text{Tr}\left(U^\dagger(t)U(t)U'^\dagger(t)\mathcal{O}'U'(t)U^\dagger(t)\mathcal{O}U(t)U'^\dagger(t)\mathcal{O}'U'(t)\right) \\ &= \text{Tr}\left(U(t)U'^\dagger(t)\mathcal{O}'U'(t)U^\dagger(t)\mathcal{O}U(t)U'^\dagger(t)\mathcal{O}'U'(t)U^\dagger(t)\right) \\ &= \text{Tr}\left(\mathcal{U}^\dagger(t)\mathcal{O}U(t)\mathcal{O}\mathcal{U}^\dagger(t)\mathcal{O}U(t)\right), \end{aligned} \quad (15)$$

where we define the error unitary $\mathcal{U}(t) = U'(t)U^\dagger(t)$. Similarly, we can modify the remaining terms of the RHS

in Eq. (14) and rewrite Eq. (13) as

$$\mathcal{I}_{\mathcal{O}}(t) = \frac{1}{2j^4} \text{Tr}(|[\mathcal{O}, \mathcal{U}^\dagger(t)\mathcal{O}U(t)]|^2). \quad (16)$$

This is the expression for error scrambling, which helps us to connect the operator incompatibility (out-of-time-order correlator) and Loschmidt echo. If the error enters through the Hamiltonian, then the error unitary for time-independent Hamiltonian becomes $\mathcal{U}(t) = e^{iH't}e^{-iHt}$ and for time-dependent kicked Hamiltonian (e.g. kicked top) $\mathcal{U}_n = U_\tau^n U_\tau^{\dagger n}$, where U_τ is the Floquet map. It is indeed remarkable that we have a rather elegant expression capturing operator incompatibility that also connects to an operational interpretation of Loschmidt echo for operators.

Understanding information gain in tomography with errors

Here, we describe information gain and the general behavior of reconstruction fidelity as shown in the main text. Later in this section, we will demonstrate the effect of the magnitude of perturbation on the fidelity obtained in tomography. We observe that independent of the degree of chaos in the dynamics, the fidelity initially rises despite errors and then starts to decline after attaining a peak. As described in the main text, we consider the density matrix of Hilbert-space dimension d that can be realized as a generalized Bloch vector \mathbf{r} by expanding $\rho_0 = I/d + \sum_{\alpha=1}^{d^2-1} r_\alpha E_\alpha$ in an orthonormal basis of traceless Hermitian operators $\{E_\alpha\}$.

The probability of reconstructing a state ρ_0 is [44]

$$p(\rho_0|\mathbf{M}, \mathcal{L}, \mathcal{M}) = A p(\mathbf{M}|\rho_0, \mathcal{L}, \mathcal{M}) p(\rho_0|\mathcal{L}, \mathcal{M}) p(\mathcal{L}, \mathcal{M}), \quad (17)$$

where A is a normalization constant. The first term $p(\mathbf{M}|\rho_0, \mathcal{L}, \mathcal{M})$, is the probability of acquiring a measurement record \mathbf{M} , given an initial state ρ_0 , the dynamics \mathcal{L} (choice of unitaries), and the measurement process \mathcal{M} (choice of operators \mathcal{O} for generating measurement record). This term contains the errors due to shot noise and helps one to quantify the signal-to-noise ratio in various directions in the operator space independent of the state to be estimated. Thus, in the limit of negligible backaction $p(\mathbf{M}|\rho_0, \mathcal{L}, \mathcal{M})$ is identical to the probability distribution corresponding to the measurement history \mathbf{M} for a given Bloch vector \mathbf{r} [39, 40, 42, 43, 60],

$$p(\mathbf{M}|\mathbf{r}) \propto \exp \left\{ -\frac{N^2}{2\sigma^2} \sum_i [M_i - \sum_\alpha \tilde{\mathcal{O}}_{i\alpha} r_\alpha]^2 \right\} \\ \propto \exp \left\{ -\frac{N^2}{2\sigma^2} \sum_{\alpha,\beta} (\mathbf{r} - \mathbf{r}_{\text{ML}})_\alpha C_{\alpha\beta}^{-1} (\mathbf{r} - \mathbf{r}_{\text{ML}})_\beta \right\}. \quad (18)$$

Therefore, this term estimates the information gained, given a density matrix, in different directions in the operator space. Now we have the second term $p(\rho_0|\mathcal{L}, \mathcal{M})$, which is the posterior probability distribution relating the knowledge of the dynamics and the measurement operators. On that account, in the limit of vanishing shot

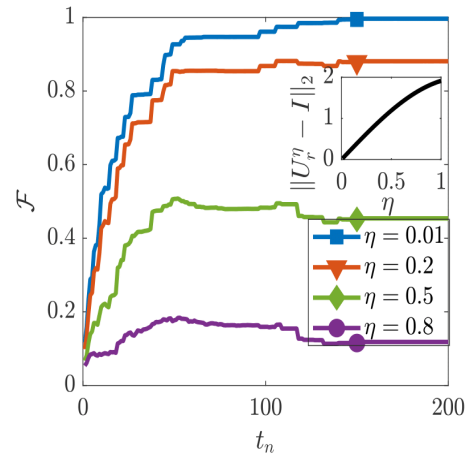


FIG. 3. Reconstruction fidelity as a function of time in the limit of vanishing shot noise for an increase in the perturbation of $\{E_\alpha\}$. The measurement operators are the perturbed ordered set $\{E'_1, E'_2, \dots, E'_k\}$ with ordered Bloch vector components of the initial state ρ_0 (i.e. that corresponds to the Bloch vector components, $r_\alpha = \text{Tr}[\rho_0 E_\alpha]$ in a particular order of their magnitudes). The perturbed operators $\{E'_\alpha\}$ are generated by applying a fractional power η of a random unitary U_r . The inset figure shows the Euclidean norm of the difference between U_r^η and Identity I , which increases with an increase in the value η .

noise and with complete knowledge of the system dynamics for given measurement observables $\{E_\alpha\}$, this conditional probability is continuously updated and ultimately becomes a product of Dirac-delta functions. Once we obtain an informationally complete measurement record, each Dirac-delta function identifies a particular Bloch vector component. The term $p(\mathcal{L}, \mathcal{M})$ in Eq. (17) can be absorbed in the constant as it gives the prior information about the choice of dynamics and measurement operators. Thus, Eq. (17) separates the probability of quantum state estimation into a product of two terms (up to a constant) [44].

$$\begin{aligned}
p(\rho_0|\mathbf{M}, \mathcal{L}, \mathcal{M}) &\propto \exp \left\{ -\frac{N^2}{2\sigma^2} \sum_i [M_i - \sum_\alpha \mathcal{O}_{i\alpha} r_\alpha]^2 \right\} p(\rho_0|\mathcal{L}, \mathcal{M}) \\
&\propto \exp \left\{ -\frac{N^2}{2\sigma^2} \sum_{\alpha, \beta} (\mathbf{r} - \mathbf{r}_{\text{ML}})_\alpha C_{\alpha\beta}^{-1} (\mathbf{r} - \mathbf{r}_{\text{ML}})_\beta \right\} p(\rho_0|\mathcal{L}, \mathcal{M})
\end{aligned} \tag{19}$$

In the limit of zero shot-noise, the errors due to the first term are zero, and we may purely focus on the conditional probability distribution, $p(\rho_0|\mathcal{L}, \mathcal{M})$. In terms of the observables in continuous measurement tomography, one can express $p(\rho_0|\mathcal{L}, \mathcal{M}) = p(\mathbf{r}|\mathcal{O}_1, \mathcal{O}_2, \dots, \mathcal{O}_n)$,

giving the conditional probability of the density matrix parameters \mathbf{r} till the time step n . For example, consider the measurement operator at the first k time steps are the ordered set $\{E_1, E_2, \dots, E_k\}$, giving precise information about Bloch vector components $\{r_1, r_2, \dots, r_k\}$. The conditional probability distribution at time k is,

$$p(\mathbf{r}|E_1, E_2, \dots, E_k) = \delta(r_1 - \text{Tr}[E_1\rho_0]) \delta(r_2 - \text{Tr}[E_2\rho_0]) \dots \delta(r_k - \text{Tr}[E_k\rho_0]) \delta\left(\sum_{\alpha \neq 1, 2, \dots, k}^{d^2-1} r_\alpha^2 = 1 - 1/d - r_1^2 - r_2^2 \dots - r_k^2\right). \tag{20}$$

Each noiseless measurement above gives us complete information in one of the orthogonal directions. For example, after the first measurement,

$$p(\mathbf{r}|E_1) = \delta(r_1 - \text{Tr}[E_1\rho_0]) \delta\left(\sum_{\alpha \neq 1}^{d^2-1} r_\alpha^2 = 1 - 1/d - r_1^2\right). \tag{21}$$

Therefore, once r_1 is determined, the rest of the $d^2 - 2$ Bloch vector components are constrained to reside on a surface given by the equation $\sum_{\alpha \neq 1}^{d^2-1} r_\alpha^2 = 1 - 1/d - r_1^2$. The state estimation procedure shall select a state based on incomplete information consistent with r_1 as determined precisely by the first measurement and the remaining Bloch vector components from a point on this surface. Therefore, qualitatively, the average fidelity of the estimated state is proportional to the area of this surface. After k time steps, the error is proportional to the area of the surface consistent with the equation $\sum_{\alpha \neq 1}^{d^2-1} r_\alpha^2 = 1 - 1/d - r_1^2 - r_2^2 - \dots - r_k^2$. This area, quantifying the average error, decreases with each subsequent measurement.

To see it in another way, consider the fidelity between the actual and reconstructed state. The fidelity $\mathcal{F} = \langle \psi_0 | \bar{\rho} | \psi_0 \rangle$,

$$\mathcal{F} = 1/d + \sum_{\alpha=1}^{d^2-1} \bar{r}_\alpha r_\alpha \tag{22}$$

Here r_α and \bar{r}_α are the Bloch vectors for ρ_0 and $\bar{\rho}$ respectively. As one makes measurements, E_1, E_2, \dots, E_k and gets information about the corresponding Bloch vector components (with absolute certainty in the case of zero

noise for example), one can express the fidelity as

$$\mathcal{F} = 1/d + \sum_{i=1}^k r_i^2 + \sum_{\alpha \neq 1, 2, \dots, k}^{d^2-1} \bar{r}_\alpha r_\alpha \tag{23}$$

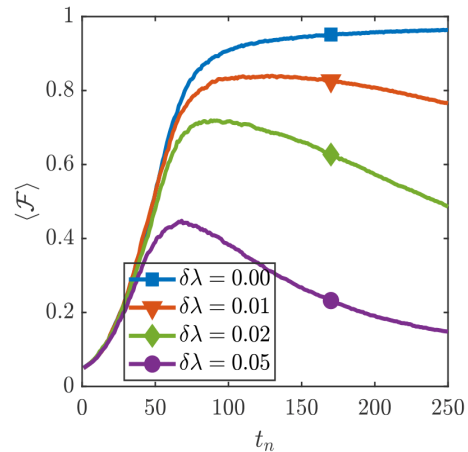


FIG. 4. Reconstruction fidelity as a function of time for an increase in perturbation strength. The measurement record is generated for spin $j = 10$. Here we consider rotation angle $\alpha = 1.4$ and kicking strength $\lambda = 7.0$ for the quantum kicked top.

The term $\sum_{i=1}^k r_i^2$ puts a lower bound on the fidelity obtained after k measurements. Here \bar{r}_α for $\alpha \neq 1, 2, \dots, k$ represent the state estimator's guess for the unmeasured Bloch vector components consistent with the constraint $(\sum_{\alpha \neq 1, 2, \dots, k}^{d^2-1} r_\alpha^2 = 1 - 1/d - r_1^2 - r_2^2 \dots - r_k^2)$. It is this guess that picks a point from the surface with an area consistent with the above constraint.

Consider the same scenario but now with perturbations to the system dynamics. The estimate of the density matrix gets modified as

$$p(\mathbf{r}|E'_1, E'_2, \dots, E'_k) = \delta(r'_1 - \text{Tr}[E'_1 \rho_0]) \delta(r'_2 - \text{Tr}[E'_2 \rho_0]) \dots \delta(r'_k - \text{Tr}[E'_k \rho_0]) \delta\left(\sum_{\alpha \neq 1, 2, \dots, k}^{d^2-1} r'^2_\alpha = 1 - 1/d - r'^2_1 - r'^2_2 \dots - r'^2_k\right). \quad (24)$$

Here, E'_1, E'_2, \dots, E'_k are the perturbed operators leading to a slightly inaccurate estimate of the Bloch vector components r'_1, r'_2, \dots, r'_k respectively. The operators $\{E'_\alpha\}$ are obtained by rotating $\{E_\alpha\}$ by a unitary U_r^η , where U_r is a random unitary and η is a fractional power which makes U_r^η close to identity. The Euclidean norm of the operator $U_r^\eta - I$ is less when η is small. Thus, η serves as the strength of perturbation in this analysis of Bloch vector components.

Despite the perturbation, the uncertainty of the Bloch vector components r_α for $\alpha \neq 1, 2, \dots, k$ reduces to the area of the surface consistent with the equation $\sum_{\alpha \neq 1, 2, \dots, k}^{d^2-1} r'^2_\alpha = 1 - 1/d - r'^2_1 - r'^2_2 \dots - r'^2_k$. The fidelity between the original and the estimated state now reads as

$$\mathcal{F} = 1/d + \sum_{i=1}^k r'_i r_i + \sum_{\alpha \neq 1, 2, \dots, k}^{d^2-1} \bar{r}_\alpha r_\alpha, \quad (25)$$

that we can see in Fig. 3. We know that the overlap between two Bloch vectors is maximum only when they are exactly aligned in the same direction, and the overlap decreases when they move far from each other. Comparing the second terms of Eq. (23) and Eq. (25) it is now clear why with an increase in perturbation, the initial rise in fidelity is less. Therefore, the drop in fidelity is more, and the fidelity saturates at a lower value if the perturbation is more, as illustrated in Fig. 4. For relatively weaker perturbations, the fidelity will continue to increase when there is an information gain despite such errors to the measurement operators. The partially inaccurate information about the j th Bloch vector owing to perturbations to the dynamics still offsets the estimator's guess of the Bloch components of the unmeasured j th direction in the operator space determined by E_j .